Proceedings of the 17th World Congress
The International Federation of Automatic Control
Seoul, Korea, July 6-11, 2008

Nonlinear Model Predictive Control of a run-of-mine ore milling circuit [⋆]

L.C. Coetzee [*] **I.K. Craig** [**] **E.C. Kerrigan** [***]

[*] *Department of Electrical, Electronic and Computer Engineering, University of Pretoria, Pretoria, 0002, South Africa. (Email: loutjie.coetzee@up.ac.za)*
[**] *Department of Electrical, Electronic and Computer Engineering, University of Pretoria, Pretoria, 0002, South Africa. (Email: icraig@postino.up.ac.za)*
[***] *Department of Aeronautics and Department of Electrical and Electronic Engineering, Imperial College London, Exhibition Road, London SW7 2AZ, United Kingdom. (Email: e.kerrigan@imperial.ac.uk)*

Abstract: In this article a nonlinear model predictive controller is presented for a run-of-mine ore milling circuit. The aim is to determine the feasibility of applying nonlinear MPC to such a circuit. The objective of the controller is to reduce the variability in the product particle size which leads to increased recovery of gold from downstream processes. The controller design is evaluated through a simulation study. *Copyright© 2008 IFAC*

Keywords: Nonlinear model predictive control, NMPC, run-of-mine ore milling circuit, ROM milling circuit

1. INTRODUCTION

Milling of ore from a mine is an important step in the metallurgical extraction process. The process is complicated by significant input and plant uncertainties, because the feed ore forms part of the grinding medium and the variation in feed ore contributes to the input uncertainty. Proper design of the milling circuit alone cannot eliminate the disturbances. Feedback control systems play an important part in reducing the effects of disturbances and increasing efficiency. Reduction of output variations does not only have a positive effect on the economics of the milling circuit itself but is also beneficial in downstream processing.

In milling circuits it is difficult to control important variables such as the product particle size, because independent control of the amount, size and hardness of the grinding medium in the mill is not possible. This causes significant uncontrollable disturbances and uncertain plant dynamics [Craig and MacLeod, 1995].

Each of the components that make up the milling circuit is highly nonlinear. Some of the components, for example the cyclone, only have nonlinear input-output relationships and no states. The cyclone model reduces to a static gain matrix when linearized.

Milling circuits have many different configurations. Being able to use the nonlinear components and arrange them in different configurations gives huge advantages in simulating different milling configurations. Applying nonlinear control like nonlinear MPC control further simplifies the process, by eliminating the need for different simulation and control models.

This study determines the feasibility of applying nonlinear MPC to the milling circuit, firstly by examining the performance of the nonlinear MPC through a simulation study. Secondly, the calculation time should be short enough for real-time implementation.

2. ROM MILL CIRCUIT

2.1 ROM Milling Circuit Description

An industrial run-of-mine ore milling circuit with single stage classification is discussed.

The circuit is fed gold-bearing ore at about 100 tons/hour and grinds it down to a product with particle size of 80% smaller than 75 μm. The ROM mill is operated in closed circuit with a hydro-cyclone that separates the product from the out-of-specification material, which is recycled to the mill. The gold is then extracted through a leaching process downstream.

A typical mill has dimensions of 5m in diameter and a length of 9m. The mill is supported by pressurized-oil circumferential bearings. The mill features lifter bars and solid white-iron liners and it is operated at 90% of critical speed [Stanley, 1987]. The mill discharges slurry through an end-discharge grate into a sump. The slurry is diluted with water in the sump and pumped to the hydro-cyclone. The hydro-cyclone has an internal diameter of 1m. The underflow of the cyclone, water and feed ore constitute the mill feed.

[⋆] The work was supported by the National Research Foundation of South Africa, grant number GUN 2069476 and MINTEK.

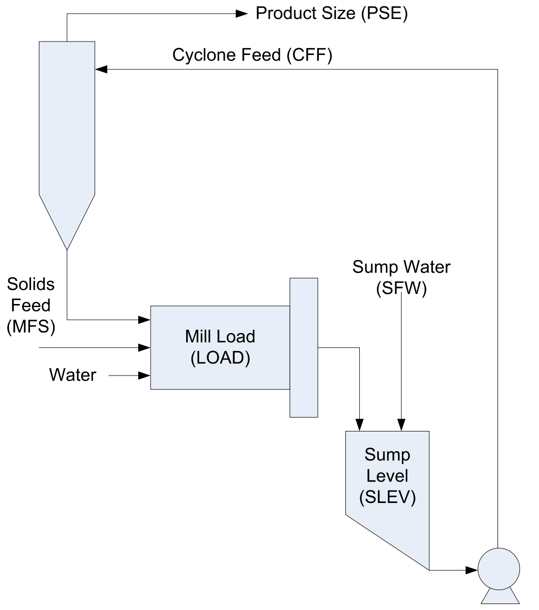

Fig. 1. Milling Circuit Schematic

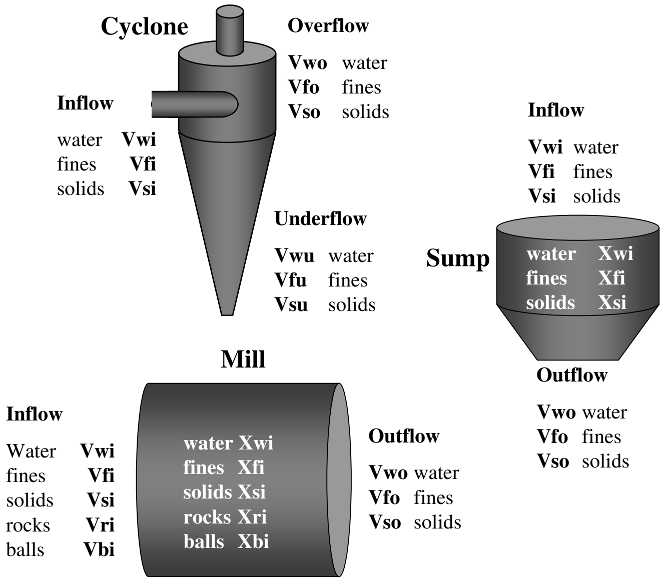

Fig. 2. Milling Circuit Modules

2.2 Milling Circuit Model

The variables of the mill (Figure 1) that can be controlled are the level of the slurry in the sump (SLEV), the product particle-size (PSE) and the mass of material in the mill (LOAD). The inputs to the mill that can be manipulated are the feed-rate of water to the sump (SFW), the flow rate of slurry to the cyclone (CFF), the feed-rate of solids to the mill (MFS) and the rate of water fed to the mill inlet (MIW).

The feed-ore consists of rock (do not discharge from the mill), coarse (out-of-specification but do discharge from the mill) and fine ore (in-specification material). The composition is described by α_f and α_r in Table 1. The circuit depicted in Figure 1 has a total of 8 states, 6 inputs and 5 outputs.

Due to brevity, the nonlinear models of each of the components in Figure 2 are not shown [Hulbert, 2005]. Only a short discussion of how the variables in Figure 2 relates to the diagram in Figure 1 will be given.

Mill module

The feed of the mill (MFS) is split into three components: volumetric flow-rate of fines (V_{fi}), volumetric flow-rate of solids (V_{si}) and volumetric flow-rate of rocks (V_{ri}) in cubic meter per hour. There are two additional feeds: volumetric flow-rate of water to the mill (V_{fi}), which relates to MIW, and volumetric flow-rate of balls to the mill (V_{bi}). The mill has five states: volume of water (X_{mw}), volume of solids (X_{ms}), volume of fines (X_{mf}), volume of rock (X_{mr}) and volume of balls (X_{mb}) in cubic meters. The mill load (LOAD) is the total of all the states. The mill only discharges solids (that also contains fines) and water through an end discharge grate (V_{wo}, V_{so}, V_{fo}). The mill model has a total of 14 parameters. Only the parameters that describe the ore hardness (η_f,ϕ_r and ϕ_b) are shown in Table 1.

Sump module

The sump module receives the discharge from the mill, which is the volumetric flow-rates of water (V_{wi}), solids (V_{si}) and fines (V_{fi}) in cubic meters per hour. The sump receives additional water ($V_{wi-sump}$), which relates to the feed-rate of water to the sump (SFW), to dilute the slurry in the sump. The discharge slurry consists of water (V_{wo}), solids (V_{so}) and fines (V_{fo}). The sump has three states: volume of water (X_{sw}), volume of solids (X_{ss}), volume of fines (X_{sf}) in cubic meters. The sump level (SLEV) is the total of all the states.

Cyclone module

The cyclone receives the slurry that consists of water (V_{wi}), solids (V_{si}) and fines (V_{fi}) from the sump. The slurry is split between the underflow and overflow such that the out-of-spec material ($V_{ci} = V_{si} - V_{fi}$) is discharged through the underflow (u) and the desired material (V_{fi}) is discharged at the overflow (o). The split is not perfect and both the underflow and overflow discharge undesired material. The fraction of desired material with regards to all solids discharged at the overflow relates to the particle size estimate (PSE $= \frac{V_{fo}}{V_{so}}$). The cyclone model has a total of 6 parameters. Only the parameters that describe the classification directly (ε_c and α_{su}) are shown in Table 1.

2.3 Objectives in Mill Control

The control of the milling circuit has multiple objectives, firstly to stabilize the system and secondly to optimize the economics of the process [Hulbert, 1989]. The economic objective is divided into sub-objectives that each contribute to the overall economic objective of the milling process. A set of possible sub-objectives for the milling circuit are to [Craig and MacLeod, 1995]:

(1) improve product quality
  (a) by increasing grind fineness,
  (b) and decreasing the fluctuations in product size,
(2) maximize throughput,
(3) minimize the amount of steel that is consumed for each ton of fines produced,

(4) and to minimize the power consumed for each ton of fines produced, etc.

The objectives above are interrelated and require trade-offs to be made. There is a trade-off between particle size of the product and the throughput of solids (objectives 1a and 2). More gold can be extracted at a finer product size (objective 1a), but the variation in particle size also influences the recovery (objective 1b).

It is assumed that the throughput of the mill is maximized when it draws maximum power from the mill motor. The $\Delta LOAD/\Delta MFS$ input-output pair is therefore often under power peak seeking control [Craig et al., 1992]. This is contrary to objective 4, which is to minimize electrical power, but given the value of the milling product versus the cost of electricity, objective 4 is considered less important.

Objectives 1 and 3 are interrelated. Steel is added to the mill to stabilize the conditions inside the mill and also increase throughput. A controller that is capable of stabilizing the particle size, will reduce the need for steel and thus objective 3 will be addressed when objective 1b is met.

A possible control strategy is to maximize throughput at a certain particle size setpoint. This strategy considers both objectives 1 and 2. The particle size setpoint may be determined by throughput targets or if throughput is not a consideration, the particle size can be optimized. A trade-off exists between throughput and grind, and grind and residue (product that is not recovered) [Craig et al., 1992]. The aim of control would be to increase throughput, while keeping grind constant.

3. NONLINEAR MODEL PREDICTIVE CONTROL

Nonlinear model predictive control (NMPC) utilizes a nonlinear model to predict the behaviour of the plant and calculate the optimal control moves or control laws with regard to a specified objective function. NMPC is derived from nonlinear optimal control over a constant or varying time interval into the future $t \in [t_k, t_k + T]$. Only the first control move or control law is implemented and a new state measurement is taken. The nonlinear optimal control problem is then recalculated for the new time interval $[t_{k+1}, t_{k+1} + T]$, which leads to receding horizon control [Mayne et al., 2000].

The nonlinear optimal control problem finds a control trajectory u such that it minimizes some scalar performance index

$$\phi_c(x, u) \tag{1}$$

subject to differential constraints

$$\dot{x}(t) = g(t, x(t), u(t)) \tag{2}$$

inequality constraints

$$\theta_c(x(t), u(t)) \leq 0 \tag{3}$$

the prescribed initial conditions

$$t_0 \triangleq 0,\ x_0 \triangleq x(t_0) \tag{4}$$

and the prescribed final conditions

$$t_f \triangleq T,\ x_f \triangleq x(t_f),\ \psi(x_f) \triangleq 0 \tag{5}$$

where $x : \mathbb{R} \to \mathbb{R}^n$ is the state trajectory, $u : \mathbb{R} \to \mathbb{R}^m$ is the control trajectory, $x(t) \in \mathbb{R}^n$ is the state vector, $\dot{x}(t) \in \mathbb{R}^n$ is the state sensitivities to time , $u(t) \in \mathbb{R}^m$ is the control vector, $x_f \in \mathbb{R}^n$ is the terminal state vector, $\phi_c(x, u) \in \mathbb{R}$ is the scalar performance function and $\theta_c(x(t), u(t)) \in \mathbb{R}^c$ is the inequality constraints function.

The nonlinear optimal control problem, consisting of a system with continuous dynamics, needs to be discretized in order to be cast in a nonlinear parameter optimization problem. This is accomplished by dividing the control interval $[0, T]$ into N discrete time intervals called nodes [Hull, 1997]

$$t_0 \triangleq 0 < t_1 < t_2 < \cdots < t_k < \cdots < t_{N-1} < t_N \triangleq T \tag{6}$$

where the sampling time is $t_s \triangleq t_{k+1} - t_k$ and N is called the prediction horizon. The functions of time $\mathbf{x}$ and $\mathbf{u}$ are replaced by their values at the nodes $x_k \in \mathbb{R}^n$ and $u_k \in \mathbb{R}^m$ for $k = 0, \ldots, N$ and some form of interpolation between nodes.

The resulting nonlinear controlled discrete-time system is

$$x_{k+1} = f_k(x_k, u_k),\ k = 0, 1, \ldots, N-1. \tag{7}$$

The nonlinear optimal control problem can now be cast into the following nonlinear parameter optimization problem

$$\min_{\substack{s_0, \ldots, s_N \\ q_0, \ldots, q_{N-1}}} \quad \phi(\mathbf{s}, \mathbf{q}) \tag{8}$$

subject to equality constraints

$$\begin{aligned} x_0 - s_0 &= 0, \\ f_i(s_i, q_i) - s_{i+1} &= 0,\ i = 0, \ldots, N-1, \end{aligned} \tag{9}$$

and inequality constraints

$$\theta_i(s_i, q_i) \leq 0,\ i = 0, \ldots, N-1, \tag{10}$$

$$\theta_N(s_N) \leq 0, \tag{11}$$

where the scalar performance index is given by

$$\phi(\mathbf{s}, \mathbf{q}) \triangleq \sum_{i=0}^{N-1} L_i(s_i, q_i) + E(s_N), \tag{12}$$

where $\phi(\mathbf{s}, \mathbf{q}) \in \mathbb{R}$ and $\theta_i(s_i, q_i) \in \mathbb{R}^c$ for all $s_i \in \mathbb{R}^n,\ i = 0, \ldots, N$ the estimated state parameters, $q_i \in \mathbb{R}^m,\ i = 0, \ldots, N-1$ the control parameters, $\mathbf{s} \triangleq (s_0, \ldots, s_N)$ the state sequence and $\mathbf{q} \triangleq (q_o, \ldots, q_{N-1})$ the control sequence to be optimized in the nonlinear optimization problem [Diehl et al., 2005].

Using only the control moves in the parameter optimization problem leads to a single integration of the state equations over the time interval $[0, T]$. If the time interval is long, the accuracy of the numerical integration is affected. The accuracy of the numerical derivatives for a given perturbation size is affected even more. To compensate for this problem, an estimate of the state value x_k at each time node is made (represented by s_k) and the system dynamics are integrated between nodes (13). This method is called direct multiple shooting [Hull, 1997]. The nonlinear optimizer then removes any error between the estimate (s_k) and actual dynamics (x_k) through the equality constraints (9).

4. NONLINEAR MODEL PREDICTIVE CONTROL IMPLEMENTATION

Implementing the nonlinear model predictive controller needs software to solve the different problems stated above. First a nonlinear optimization software is required, to solve the nonlinear parameter optimization problem stated in (8). The software used is a package called IPOPT [Kawajir et al., 2006], which is used for large scale sparse nonlinear optimization problems.

IPOPT requires the following functions to be provided:

- Scalar performance function value $\varphi(X)$
- Gradient of the performance function $\nabla\varphi(X)$
- Constraint functions values $\vartheta(X)$
- Jacobian of the constraints $\nabla\vartheta(X)$
- (optionally) Hessian of the Lagrangian function $\sigma_f \nabla^2\varphi(X) + \sum_{i=1}^{m} \lambda_i \nabla^2\vartheta_i(X)$

where X is the vector of all decision variables. For the problem specified in (8)-(12), the vector of decision variables is defined as $X \triangleq (s_0, q_0, \ldots, s_{N-1}, q_{N-1}, s_N) \in \mathbb{R}^{((n+m)\cdot N+n)}$.

The equality constraint functions contains discretized system dynamics $f_k(x_k, u_k)$. For a continuous system, the interpolation between nodes are done by integrating the state equations (2) for one sample time t_s

$$x_{k+1} \triangleq f_k(x_k, u_k) \triangleq \int_{t_k}^{t_k+t_s=t_{k+1}} g(\tau, x(\tau), u_k)\, d\tau \tag{13}$$

with the initial conditions $x(t_k) = x_k = s_k$ and the controls $u_k = q_k$ constant over the interval $[t_k, t_{k+1}]$.

The scalar performance function is defined as

$$\varphi(X) \triangleq \sum_{i=0}^{N-1} L_i(s_i, q_i) + E(s_N) \tag{14}$$

where the scalar interval performance indexes and the terminal performance index can be given by a quadratic function

$$\begin{aligned} L_i(s_i, q_i) &\triangleq \int_{t_i}^{t_i+t_s} x_i^T(\tau) Q x_i(\tau) + q_i^T R q_i \; d\tau, \\ & \qquad i = 0, \ldots, N-1, && (15) \\ E(s_N) &\triangleq s_N^T P s_N, && (16) \end{aligned}$$

where Q and R represent the weighting matrices on the states and controls respectively and P is the terminal cost weighting matrix. The state value is obtained by integrating (2)

$$x_i(t) \triangleq \int_{t_i}^{t} g(\tau, x(\tau), u_i)\, d\tau \tag{17}$$

where the initial state vector is $x_i(t_i) = s_i$ and the constant control vector is $u_i = q_i$. The integration of (15) and (17) is done simultaneously by a software package called SUNDIALS [Hindmarsh and Serban, 2006], where (17) is the solution of the main ODEs defined in the node interpolation (13), while (15) is solved as a quadrature function.

The gradient of the performance function $\nabla\varphi(X) \in \mathbb{R}^{((n+m)\cdot N+n)}$ then becomes

$$\nabla\varphi(X) = \begin{bmatrix} \frac{\partial L_0(s_0,q_0)}{\partial s_0} \\ \frac{\partial L_0(s_0,q_0)}{\partial q_0} \\ \vdots \\ \frac{\partial L_{N-1}(s_{N-1},q_{N-1})}{\partial s_{N-1}} \\ \frac{\partial L_{N-1}(s_{N-1},q_{N-1})}{\partial q_{N-1}} \\ \frac{\partial E(s_N)}{\partial s_N} \end{bmatrix}. \tag{18}$$

The values of the constraint functions $\vartheta(X)$ are interleaved equality and inequality constraint functions with the same decision variables that will result in a Jacobian of the constraints $\nabla\vartheta(X)$ that is sparse and banded. For NMPC, the following structure for the constraints function $\vartheta(X) \in \mathbb{R}^{((n+c)\cdot N+n)}$ is presented

$$\vartheta(X) \triangleq \begin{bmatrix} x_0 - s_0 \\ \theta_0(s_0, q_0) \\ f_0(s_0, q_0) - s_1 \\ \theta_1(s_1, q_1) \\ f_1(s_1, q_1) - s_2 \\ \vdots \\ \theta_{N-1}(s_{N-1}, q_{N-1}) \\ f_{N-1}(s_{N-1}, q_{N-1}) - S_N \\ \theta_N(s_N) \end{bmatrix} \tag{19}$$

that results in a Jacobian of the constraints function $\nabla\vartheta(X) \in \mathbb{R}^{((n+c)\cdot N+n)\times((n+m)\cdot N+n)}$ shown in Figure 3. IPOPT only requires the non-zero entries to be populated for this sparse Jacobian matrix. The number of non-zero entries for this structure is nnzje $= (n + c\cdot(n+m) + n\cdot(n+m))\cdot N + n$.

SUNDIALS is also capable of calculating forward sensitivities and adjoint sensitivities. This is useful for calculating the sensitivities of the system dynamics $f_k(x_k, u_k)$ as well as the stage costs $L_k(x_k, u_k)$, $k = 0, \ldots, N-1$ with regards to initial states $x(t_k) = s_k$ and inputs $u_k = q_k$.

The sensitivities of differential equations (2) with regards to the states $\frac{\partial g(t,x,u)}{\partial x} \in \mathbb{R}^{n\times n}$ and inputs $\frac{\partial g(t,x,u)}{\partial u} \in \mathbb{R}^{n\times m}$ requires software that does numeric differentiation. For this purpose, a software package called CPPAD of the COIN-OR project [Lougee-Heimer, 2003] is used. It does Automatic Differentiation of specially modified C++ code. It works by recording all the mathematical operations being done in the desired function and then uses the chain rule of differentiation to calculate the derivatives. The advantages of Automatic Differentiation is that it is fast to calculate and does not suffer from truncation errors present in other numerical methods.

5. SIMULATION

A simulation study is shown where the nonlinear model predictive controller of section 3 is applied to the ROM milling model presented in section 2.

In this simulation scenario the "actual" plant differs from the nominal model. The parameters of the milling circuit have large uncertainties, especially the parameters relating to the composition of the feed-ore and the hardness of the

$$\nabla\vartheta(X) = \begin{bmatrix} -\mathbb{I} & 0 & 0 & 0 & 0 & 0 \\ \frac{\partial\theta_0(s_0,q_0)}{\partial s_0} & \frac{\partial\theta_0(s_0,q_0)}{\partial q_0} & 0 & 0 & 0 & 0 \\ \frac{\partial f_0(s_0,q_0)}{\partial s_0} & \frac{\partial f_0(s_0,q_0)}{\partial q_0} & -\mathbb{I} & 0 & 0 & 0 \\ 0 & 0 & 0 & 0 & 0 & 0 \\ 0 & 0 & 0 & 0 & 0 & 0 \\ \vdots & \vdots & \ddots & \vdots & \vdots & \vdots \\ 0 & 0 & 0 & 0 & 0 & 0 \\ 0 & 0 & 0 & -\mathbb{I} & 0 & 0 \\ 0 & 0 & 0 & \frac{\partial\theta_{N-1}(s_{N-1},q_{N-1})}{\partial s_{N-1}} & \frac{\partial\theta_{N-1}(s_{N-1},q_{N-1})}{\partial q_{N-1}} & 0 \\ 0 & 0 & 0 & \frac{\partial f_{N-1}(s_{N-1},q_{N-1})}{\partial s_{N-1}} & \frac{\partial f_{N-1}(s_{N-1},q_{N-1})}{\partial q_{N-1}} & -\mathbb{I} \\ 0 & 0 & 0 & 0 & 0 & \frac{\partial\theta_N(s_N)}{\partial s_N} \end{bmatrix}.$$

Fig. 3. Jacobian of the constraints.

Table 1. Parameter values for a ROM milling circuit.

	Nominal	Min	Max	%Δ	Description
α_f	0.09	0	0.2	30	Feed Ore - Fraction fines
α_r	0.04	0	0.1	30	Feed Ore - Fraction rocks
η_f	28	17	40	30	Mill - Power per fines produced [kW hr / ton]
ϕ_r	187	90	280	30	Mill - Rock abrasion factor [kW hr / ton]
ϕ_b	94	70	120	15	Mill - Steel abrasion factor [kW hr / ton]
ε_c	184	147	220	5	Cyclone - Coarse split
α_{su}	0.16	0.13	0.2	5	Cyclone - Fraction solids in underflow

ore (energy needed to grind a ton of ore). The parameter variations used in the simulation study are shown in Table 1. The parameter variations are time-varying and assumed to be uniformly distributed between the bounds. The prediction model of the nonlinear model predictive controller uses the nominal parameter values.

The milling circuit is simulated at the operating point as described in Table 2. The constraints of the milling circuit is also described in Table 2. The simulation is done for 260 minutes with a recommended sampling time of 10 seconds. A prediction horizon of 24 is used to predict behaviour over 240 seconds, resulting in 344 decision variables as part of the optimization problem.

A disturbance is introduced in the feed-ore. At time 20 minutes, the amount of rock in the feed-ore is increased by 30% and at time 100 minutes, the hardness of the ore is increased by 25%.

The mill level (LOAD), as shown in Figure 4, is given highest priority and the controller keeps the level constant. The particle size (PSE), as shown in Figure 4, is given secondary priority. The PSE shows a small drop from the setpoint of 80% when the ore hardness increases. The sump level (SLEV), as shown in Figure 4, is given least priority, which results in it showing large variations.

Figure 5 shows the flow-rate of water to the sump, flow-rate of slurry to the cyclone and flow-rate of feed-ore to the circuit that the controller is manipulating.

The simulation executed with an average time of about 4 seconds per iteration, which is well below the recommended sampling time of 10 seconds.

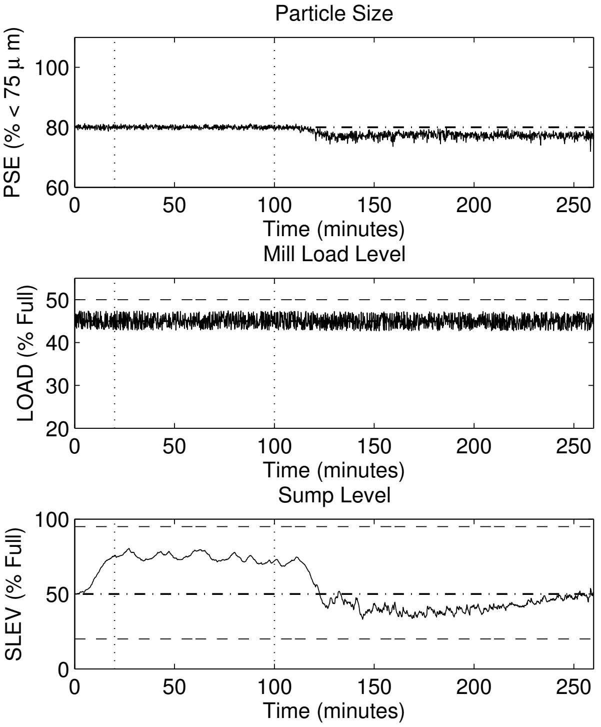

Fig. 4. Controlled Variables.
The dashed lines indicate the constraints on the variable and the vertical dotted lines indicate the start of the disturbance events. The dash-dot line indicates the setpoint.

6. CONCLUSIONS

The nonlinear MPC performed well in the simulation study. It tracked the operating point very well despite disturbances in the feed-ore.

Extending this work, a robust nonlinear MPC can be applied, which builds on linear robust MPC done by Coetzee and Craig [2007], which explicitly incorporates the description of common disturbances, for example the spillage water being dumped in the sump as well as the parameter uncertainties, such as those described in Table 1.

Table 2. Constraints and operating point.

Variable	Min	Max	Operating Point	Description
X_{mw}	0 m^3	50 m^3	8.53 m^3	The holdup of water in the mill
X_{mc}	0 m^3	50 m^3	9.47 m^3	The holdup of coarse ore in the mill
X_{mf}	0 m^3	50 m^3	3.54 m^3	The holdup of fine ore in the mill
X_{mr}	0 m^3	50 m^3	20.25 m^3	The holdup of rock in the mill
X_{mb}	0 m^3	20 m^3	6.75 m^3	The holdup of balls in the mill
X_{sw}	0 m^3	10 m^3	3.95 m^3	The holdup of water in the sump
X_{sc}	0 m^3	10 m^3	1.05 m^3	The holdup of coarse ore in the sump
X_{sf}	0 m^3	10 m^3	0.14 m^3	The holdup of fine ore in the sump
MIW	$0\ \frac{\mathrm{m}^3}{\mathrm{hour}}$	$100\ \frac{\mathrm{m}^3}{\mathrm{hour}}$	$33.33\ \frac{\mathrm{m}^3}{\mathrm{hour}}$	The flow-rate of water to the circuit.
MFS	$0\ \frac{\mathrm{tons}}{\mathrm{hour}}$	$200\ \frac{\mathrm{tons}}{\mathrm{hour}}$	$100\ \frac{\mathrm{tons}}{\mathrm{hour}}$	The flow-rate of ore to the circuit (consists of rocks, coarse and fine ore).
V_{bi}	$0\ \frac{\mathrm{tons}}{\mathrm{hour}}$	$4\ \frac{\mathrm{tons}}{\mathrm{hour}}$	$2\ \frac{\mathrm{tons}}{\mathrm{hour}}$	The flow-rate of balls to the circuit.
$\alpha_{millspeed}$	0.7	1.0	0.82	The fraction of critical mill speed.
CFF	$400\ \frac{\mathrm{m}^3}{\mathrm{hour}}$	$500\ \frac{\mathrm{m}^3}{\mathrm{hour}}$	$442.59\ \frac{\mathrm{m}^3}{\mathrm{hour}}$	The flow-rate of water from the sump to the cyclone.
SFW	$0\ \frac{\mathrm{m}^3}{\mathrm{hour}}$	$400\ \frac{\mathrm{m}^3}{\mathrm{hour}}$	$266.67\ \frac{\mathrm{m}^3}{\mathrm{hour}}$	The flow-rate of extra water to the sump.
LOAD	30 m^3	50 m^3	45 m^3	The total charge of the mill. Must not be fuller than 50%.
SLEV	2 m^3	9.5 m^3	5.0 m^3	The level of the sump. Should not run empty and also not overflow.
Rheology	0	1	0.51	Describes the fluidity of the slurry in the mill, where 1 is water and 0 represents a "thick mud" that does not flow.

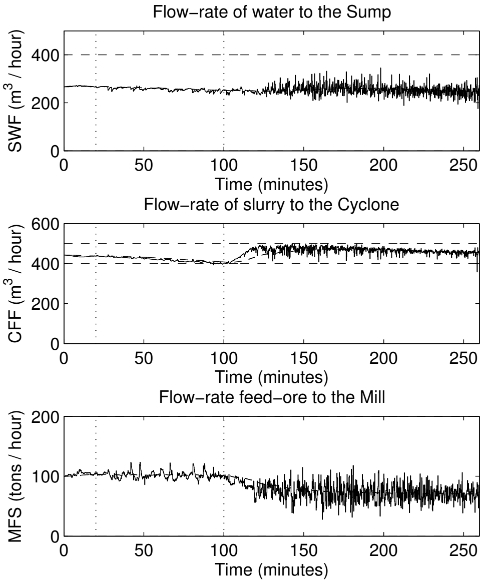

Fig. 5. Manipulated Variables.
The dashed lines indicate the constraints on the variable and the vertical dotted lines indicate the start of the disturbance events. The dash-dot line indicates the setpoint.

The simulation further assumed full-state feedback. It is necessary to add an observer to the loop to evaluate practical feedback scenarios.

The simulation shows that the computational time falls within the sampling time. Increasing the prediction horizon significantly increases the calculation time. Tuning the controller will include the selection of the prediction horizon for stability and performance, while maintaining a reasonable calculation time.

REFERENCES

L.C. Coetzee and I.K. Craig. Robust MPC of a run-of-mine ore milling circuit. In *7^th IFAC Symposium on Nonlinear Control Systems, 21-24 August*, pages 904–909, Pretoria, South Africa, August 2007.

I. K. Craig and I. M. MacLeod. Specification framework for robust control of a run-of-mine ore milling circuit. *Control Engineering Practice*, 3(5):621–630, 1995.

I. K. Craig, D. G. Hulbert, G. Metzner, and S. P. Moult. Optimized multivariable control of an industrial run-of-mine milling circuit. *Journal of the South African Institute of Mining and Metallurgy*, 92(6):169–176, June 1992.

M. Diehl, H. G. Bock, and J. P. Schloder. A real-time iteration scheme for nonlinear optimization in optimal feedback control. *SIAM Journal on Control and Optimization*, 43(5):1714–1736, 2005.

A. C. Hindmarsh and R. Serban. *User Documentation for CVODES v2.5.0.* Center for Applied Scientific Computing Lawrence Livermore Laboratory, November 2006.

D. G. Hulbert. The state of the art in the control of milling circuits. In *6th IFAC Symposium on Automation in Mining, Mineral and Metal Processing (Buenos Aires)*, 1989.

D. G. Hulbert. Models for mill circuit simulation. Private Communication, September 2005. MINTEK.

D. G. Hull. Conversion of Optimal Control Problems into Parameter Optimization Problems. *Journal of Guidance, Control, and Dynamics*, 20(11):57–60, 1997.

Y. Kawajir, C. Laird, and A. Wachter. *Introduction to Ipopt: A tutorial for downloading, installing, and using Ipopt, Revision: 799.* Carnegie Mellon University, Pittsburgh, PA, USA, November 2006. URL `https://projects.coin-or.org/Ipopt`.

R. Lougee-Heimer. The Common Optimization INterface for Operations Research. *IBM Journal of Research and Development*, 47(1):57–66, January 2003. URL `http://www.coin- or.org/CppAD/`.

D. Q. Mayne, J. B. Rawlings, C. V. Rao, and P. O. M. Scokaert. Constrained model predictive control: Stability and optimality. *Automatica*, 36:789–814, 2000.

G. G. Stanley. The Extractive Metallurgy of Gold in South Africa. Technical Report Vol 1, South African Institute of Mining and Metallurgy, Johannesburg, 1987.